ORIGINAL PAPER

Binding of rhodamine B and kiton red S to cucurbit[7]uril: density functional investigations

**Jayshree K. Khedkar · Krishna K. Jagtap ·
Rahul V. Pinjari · Alok Kumar Ray · Shridhar P. Gejji**

Abstract The binding of the laser dyes rhodamine B (RhB) and sulforhodamine B (kiton red S or KRS) to a cucurbit[7]uril (CB[7]) host has been investigated using density functional theory. Both guests (RhB and KRS) contain two N,N-diethylamino groups on a xanthene core. The lowest-energy structure of these host–guest complexes has one of the N,N-diethylamino groups encapsulated within the host cavity, that engenders C–H···O interactions with portals, while the remaining noninteracting diethylamino group resides outside the cavity. The ^{1}H NMR chemical shifts derived using the gauge-independent atomic orbital method are consistent with those observed in experiments.

Keywords Cucurbit[n]uril · Rhodamine B · KRS · ^{1}H NMR · Density functional

Introduction

The growing interest in the cucurbit[n]uril (CB[n]) family (n=6–8) as novel hosts in supramolecular chemistry can be attributed to their unusual and distinct molecular recognition properties [1]. Structural features such as hydrophilic portals

J. K. Khedkar · R. V. Pinjari · S. P. Gejji (✉)
Department of Chemistry, University of Pune,
Pune 411 007, India
e-mail: spgejji@chem.unipune.ac.in

K. K. Jagtap · A. K. Ray
Laser & Plasma Technology Division,
Bhabha Atomic Research Centre,
Mumbai 400 085, India

and a hydrophobic cavity make these novel systems fascinating molecular containers for entrapping neutral as well as positively charged guest molecules with efficient and selective binding [2]. Binding ability, photophysical behavior and salt effect during complexation of calix[4]arene, β-cyclodextrin and CB[7] macrocycles with fluorescent guests such as rhodamine B, neutral red and acridine red [3] are investigated in the recent literature. Interaction studies of xanthene-based cationic fluorescent dye molecules with CB[7] in water have stimulated significant interest, as reflected by the recent literature [4, 5]. The molecular encapsulation of organic dyes within molecular containers such as cyclodextrins and cucurbit[n]urils is an attractive supramolecular strategy due to the flexible nature of these hosts and relatively rapid synthetic process which protects confined guest molecule from aggregation or photochemical degradation [6]. Moreover, UV-visible absorption spectral measurements, ^{1}H NMR, and fluorescence titration [7] experiments have focused on the RhB@CB[7] complexes that result from placing aqueous CB[7] in the presence of monocationic xanthene dye. It has been shown that adding CB[7] to an aqueous solution of RhB or KRS results in improved photostability and thermo-optical properties [8]. Fluorescence titration experiments by Mohanty and coworkers [8] indicated that both RhB and KRS form 1:1 complexes in the presence of CB[7]. Thus, gaining a molecular level understanding of the host–guest interactions in CB[7] complexed with the laser dyes RhB and KRS is an interesting and useful pursuit. It is well known that host–guest binding, primarily hydrogen bonding and electrostatic interactions, are governed by cavity size and the hydrophobicity of the CB[n] cavity. Recent work by Gejji and coworkers [9] demonstrated how the electron charge distribution derived from the topography of the molecular electrostatic potential (MESP) can be used to gauge the shapes and dimensions of the cavities of CB[n] homologs. CB[7] possesses a near-
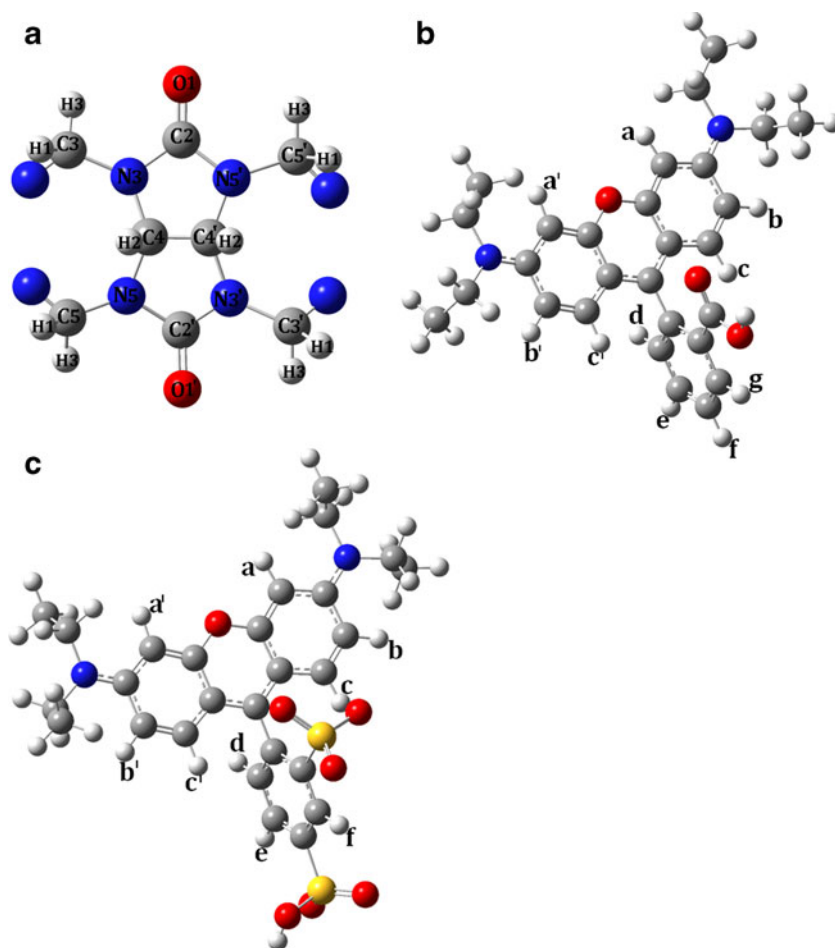
circular cavity with an effective diameter of 7.11 Å and a cavity height of 7.63 Å, so it is capable of encapsulating a variety of organic molecules [10].

In the present paper, to understand the interactions between the laser dyes RhB or KRS and the CB[7] macrocycle (cf. Fig. 1), we derived the electronic structures of their complexes using density functional theory. Both guests (RhB and KRS) possess interesting molecular attributes, with the charge being delocalized along the molecular axis, which has terminal diethyl amino groups. These dyes differ only in their pendant phenyl substituents; RhB possesses a carboxylic acid (CO_2H) group at the *ortho* position of the pendant phenyl ring, while KRS has sulfonic groups (SO_3H) at the *ortho* and *para* positions. Below, we analyze how this substitution engenders different host–guest binding patterns for RhB or KRS when complexed with a CB[7] host.
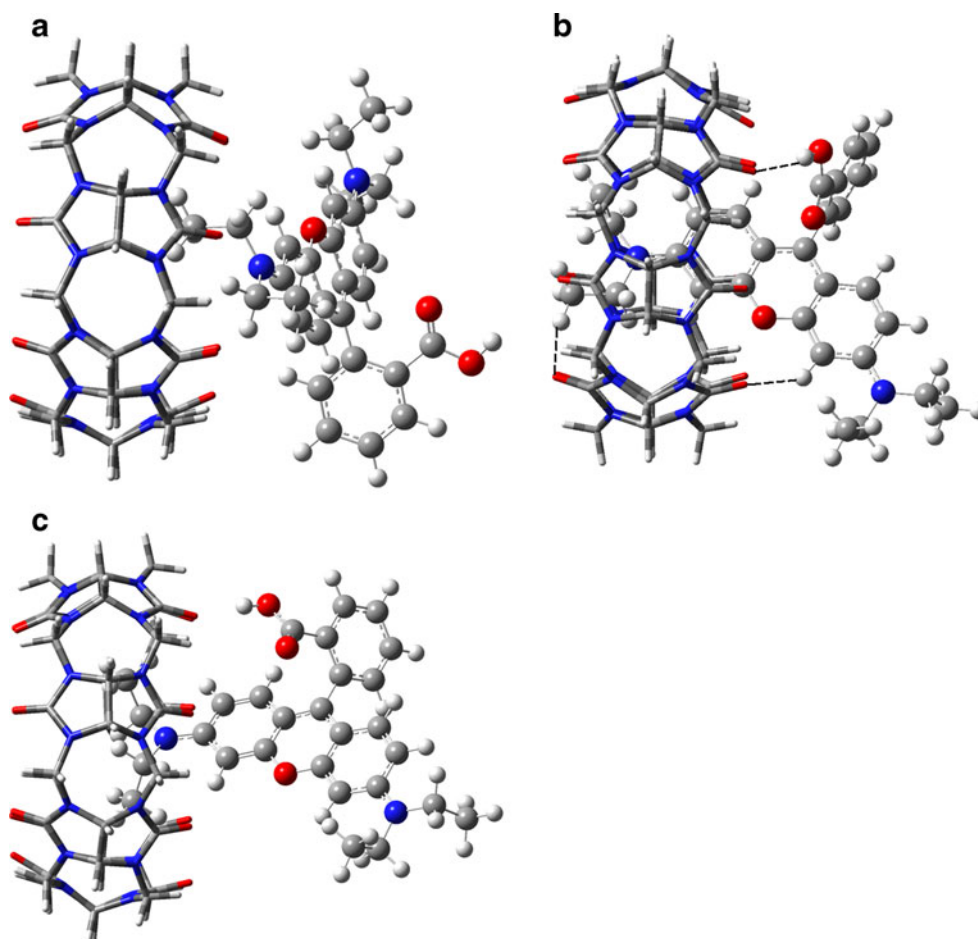
Computational methods

The structure and the atom numbering scheme in the glycouril monomer of CB[7] is depicted in Fig. 1, along with

those for the dyes RhB and KRS. Geometry optimizations of CB[7], RhB, KRS, and the host–guest complexes RhB@CB[7] and KRS@CB[7] with different binding patterns were carried out using the GAUSSIAN 09 suite of programs [11]. Accordingly, six complex structures of RhB@CB[7] and four different complex structures of KRS@CB[7] were generated, in which one *N,N*-diethyl amino end of the RhB or KRS guest was (a) encapsulated within the host cavity, (b) partially encapsulated in the cavity of CB[7], or (c) interacted laterally with portal oxygens of the CB[7] host. These are shown schematically in Figs. 1S and 2S of the "Electronic supplementary material" (ESM). The RhB@CB[7] and KRS@CB[7] conformers were optimized within the framework of density functional theory incorporating Becke's three-parameter exchange augmented by Lee, Yang, and Parr's (B3LYP) correlation functional [12, 13], employing the 6-31G(d,p) basis set. Relative stabilization energies ΔE_{rel} were calculated by subtracting the electronic energy of the dye@CB[7] conformer of interest from the lowest-energy dye@CB[7] conformer. The binding energy ΔE_{bind} was obtained by subtracting the sum of the electronic energies of the host and the guest from that of the complex. The energies thus obtained were

Fig. 1 Optimized geometries of **a** the glycouril unit of CB[7], **b** rhodamine B (RhB), and **c** sulforhodamine B (KRS). Atom numbering is also shown

Fig. 2 "A", "B", and "C" conformers of RhB@CB[7] with different host–guest binding patterns

corrected for host and guest deformation during complex formation. Accordingly, the deformation correction for an individual host (or guest) was calculated by subtracting the electronic energy of the host (or guest) in the complex from that of the isolated host (or guest). NMR chemical shifts (δ) were obtained by subtracting the nuclear magnetic shielding tensors of the protons in RhB, KRS, and CB[7] from those in tetramethylsilane (used as a reference), employing the gauge-independent atomic orbital (GIAO) method [14]. The effect of solvation on the proton chemical shifts (δ_H) for the complexes was modeled through self-consistent reaction field (SCRF) theory, incorporating the polarizable continuum model [15]. The ^{1}H NMR chemical shifts thus obtained for CB[7] complexed with RhB or KRS guests were compared to those obtained experimentally [7, 8, 16], which ultimately led to a molecular-level understanding of the host–guest interaction patterns and whether the guest is encapsulated within the cavity or interacts laterally with host portals.

Results and discussion

The RhB@CB[7] conformers displayed in Fig. 2 reveal three distinct local minima, corresponding to the binding

of one of the 3,6-N,N-diethylamino groups of guest by (a) interacting laterally with portals ("A" in Fig. 2a), (b) penetrating within the cavity and engendering interactions with ureido oxygens of the upper rim of the host ("B" in Fig. 2b), and (c) becoming confined within the host cavity, with the remaining noninteracting group excluded from the cavity ("C" in Fig. 2c). The stabilization energies (in kJ mol^{-1}) relative to the lowest energy complex are given in Table 1, along with

Table 1 Relative stabilization energies, deformation energies, and binding energies (ΔE_{bind}, incorporating the deformation correction) in kJ mol^{-1} of RhB@CB[7] and KRS@CB[7] optimized at the B3LYP/6-31G(d,p) level

	ΔE_{rel}	ΔE_{def}			ΔE_{bind}
		CB[7]	Dye	Dye+CB[7]	
Dye RhB					
"A"	0.00	4.7	8.6	13.3	133.4
"B"	0.65	12.8	24.0	36.8	156.2
"C"	14.02	9.0	28.7	37.6	143.7
Dye KRS					
"A"	0.00	16.0	10.0	26.0	176.7
"B"	68.98	32.0	58.2	90.2	178.2

the binding energies for these complexes. As shown, conformer "B" of RhB@CB[7] was found to be ~22.8 kJ mol^{-1} lower in energy than "A" (133.4 kJ mol^{-1}). It may therefore, be conjectured that the encapsulation of RhB within CB[7] is favored over lateral interactions of RhB with host portals, which can be partly attributed to the strength and number of hydrogen-bonding interactions involved in each case. The RhB@CB[7] complex in its lowest-energy structure ("B") exhibits two C–H···O interactions involving the ethyl group of the guest in addition to O–H···O interactions between the hydroxyl and portal oxygens. KRS@CB[7] conformers with one N,N-diethylamino group either interacting laterally with ("A") or encapsulated ("B") within the cavity of CB[7] via C–H···O interactions are displayed in Fig. 3. As shown in Table 1, the calculated binding energies of KRS to CB[7] in conformers "A" (176.7 kJ mol^{-1}) and "B" (178.2 kJ mol^{-1}) are comparable.

Selected geometrical parameters for CB[7] and the RhB@CB[7] and KRS@CB[7] complexes are reported in Table 2. The C3–N3 bond distance is predicted to be 0.004 Å longer in the RhB@CB[7] complex than in the isolated CB[7] host, while the remaining bond distances in the glycouril monomer are almost unchanged. Accommodating one of the N,N-diethylamino groups within the host cavity leads to decreased separation (8.307 Å, versus 8.530 Å in the isolated host) of radially opposite ureido oxygens from the upper rim (which interact with the diethylamino group from the guest). Further, when the separation between the ureido oxygens in the upper rim of CB[7] is the smallest, the oxygens in the lower rim of corresponding glycouril units show the largest separation, and vice versa. The ureido oxygens of the upper rim from the neighboring glycouril units of CB[7] move closer on complexation (3.782 Å, versus 3.800 Å before complexation), as shown in Table 2. Generally, bond angles vary maximally within 1° than those in the isolated CB[7] host. Interaction between the N,N-diethylamino group of RhB and CB[7] leads to significant distortion of the host cavity, and the methylene groups of the glycouril monomers deviate significantly from planarity. As shown in Fig. 3b (the "B" conformer), the KRS@CB[7] complex presents two C–H···O interactions. Encapsulation of one of the N,N-diethylamino groups of KRS within the cavity of CB[7] results in decreased separation of the radially opposite ureido oxygens in both the upper and lower rims (8.491 and 8.375 Å) compared to the isolated CB[7] host (8.530 Å). The C2–N3 distance is predicted to be 1.385 Å in the complex, compared to 1.393 Å in free CB[7]. Changes in the remaining bond distances in CB[7] upon the encapsulation of KRS are within 0.006 Å. Moreover, such interactions with the KRS guest move the ureido oxygens from the upper and lower rims of the neighboring glycouril units closer to each other (3.749 and 3.779 Å) than in the isolated CB[7] host (3.800 Å). The bond angles in KRS@CB[7] change by less than 2° upon complexation, and the dihedral angles O1–C2–N3–C3 and O1–C2–N5′–C5′ deviate by 3° at most.
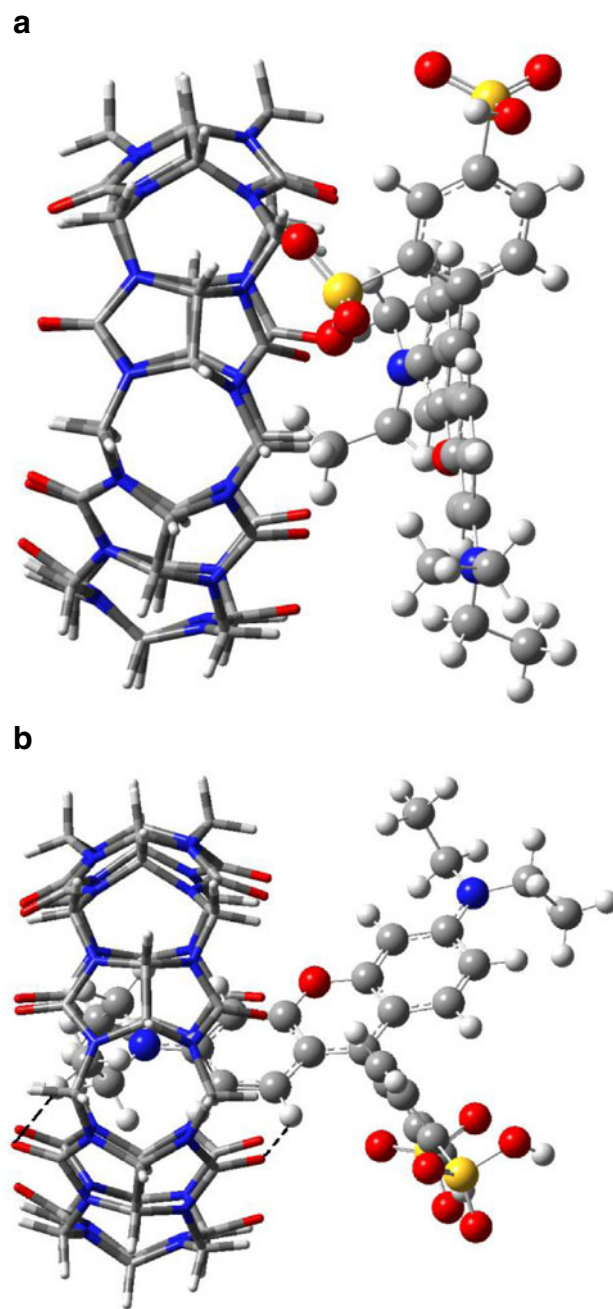

Fig. 3 A and B conformers of KRS@CB[7], as obtained from B3LYP theory

The HOMO and LUMO frontier orbitals of the RhB@CB[7] and KRS@CB[7] complexes are displayed in Figs. 4 and 5, respectively, using isosurfaces of 0.02 au. It is clear that the electron-rich region of the highest occupied molecular orbital (HOMO) of CB[7] resides largely on the glycouril rings. On complexation with RhB, the electron-rich region relocates to the xanthene core. The HOMO of the RhB@CB[7] complex resides on the xanthene core with the N,N-diethylamino substituent, whereas the lowest unoccupied molecular orbital (LUMO) extends out to the pendant aromatic ring too.

Table 2 Selected bond distances (in Å) and bond angles (in °) in CB[7], RhB@CB[7], and KRS@CB[7]

	CB[7]	RhB@CB[7]	KRS@CB[7]
O1–C2	1.213	1.215	1.224
C2–N3	1.393	1.395	1.385
N3–C3	1.446	1.450	1.450
N3–C4	1.446	1.447	1.452
C4–C4′	1.570	1.569	1.565
C3–H1	1.101	1.101	1.096
C4–H2	1.102	1.101	1.096
C3–H3	1.093	1.092	1.090
O–O[a]	8.530	8.574 (8.307)	8.375 (8.491)
O_1O_1*[b]	3.800	3.864(3.782)	3.779 (3.749)
O1–C2–N3	126.4	126.3	126.0
C2–N3–C3	121.1	121.4	121.8
C2–N3–C4	112.8	113.0	112.3
N3–C4–C4	103.4	103.3	103.4
N3–C2–N5	107.2	107.3	109.0
C3–N3–C4	125.0	123.3	123.9
N3–C4–N5	117.0	116.8	115.8
O1–C2–N3–C3	−5.3	−11.9	−8.1
O1–C2–N5′–C5′	5.3	6.4	8.4
C2–N3–C4–N5	−116.5	−109.2	−115.2
C2–N3–C4–C4′	−3.5	−8.6	−5.6
C2–N3–C3–H3	−4.4	−12.7	−6.7

Figures in parentheses denote distances between the oxygens in the upper rim, which interacts with the diethylamino group of the guest

[a] Separation between the radially opposite oxygens of the portals of CB[7]

[b] Separation between the two oxygens in adjacent glycouril units

Furthermore, the HOMOs of the RhB@CB[7] complex and isolated RhB are strikingly similar. On the other hand, the HOMO of the KRS@CB[7] complex show electron-rich regions on the SO_3^- group whereas LUMO resides on the xanthene core. The HOMO–LUMO energy difference was calculated to be 2.86 eV for isolated RhB versus 2.94 eV for its complex with CB[7]. For isolated KRS, this energy gap was found to be 2.48 eV, and this value decreased by 0.25 eV on complexation. Thus, the HOMO–LUMO energy difference for the RhB@CB[7] complex was predicted to be nearly 0.70 eV larger than that for KRS@CB[7].

The net atomic charges in the host–guest complexes, obtained from the molecular electrostatic potential, are given in Table 3. Thus complexation of CB[7] with RhB causes the charge on the oxygen participating in O–H···O interaction to be −0.379 au, compared to −0.452 and −0.435 au for the oxygens facilitating C–H···O interactions at CB[7] portals. Moreover, noninteracting portal oxygens have a net charge of −0.426 au in the complex. The residual charge on the nitrogen atom of the N,N-diethylamino group encapsulated within the cavity of CB[7] is predicted to be −0.507 au, as compared to −0.457 au for the isolated guest. On the other hand, in case of the KRS@CB[7] complex, the net atomic charges for the oxygens participating in C–H···O interactions are found to be −0.419 au and −0.387 au. Thus, it may be conjectured that the KRS@CB[7] complex, which does not exhibit O–H···O interactions, possesses stronger C–H···O interactions than those in RhB@CB[7].

It is known that the solvent has a profound influence on the NMR chemical shifts (δ_H) of protons that do not participate in hydrogen-bonding host–guest interactions [17]. We therefore derived the δ_H values of the complexes along with those of the

Fig. 4 HOMOs and LUMOs (displayed using isosurfaces of 0.02 au) of CB[7], RhB, and RhB@CB[7]
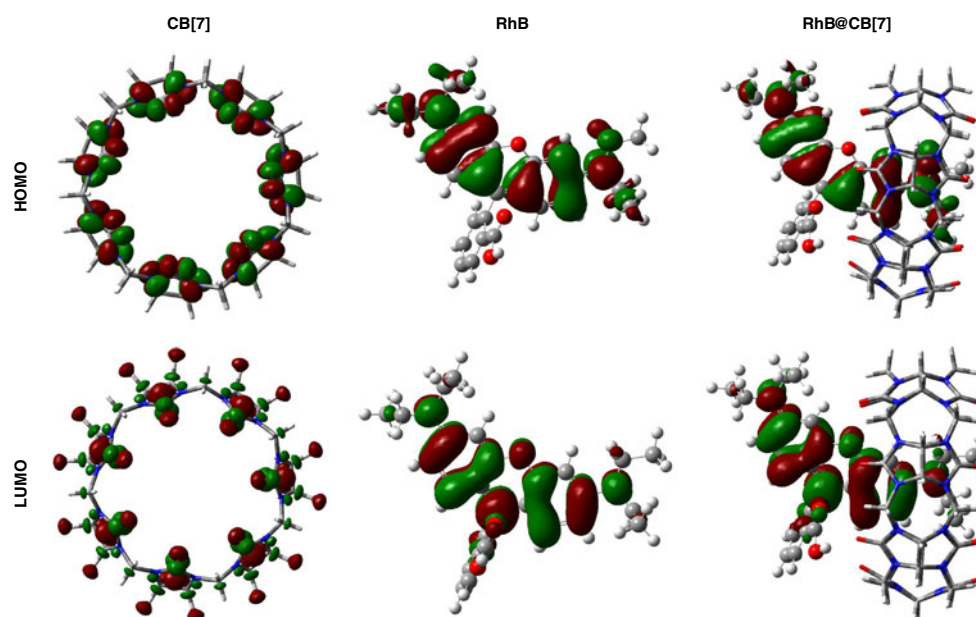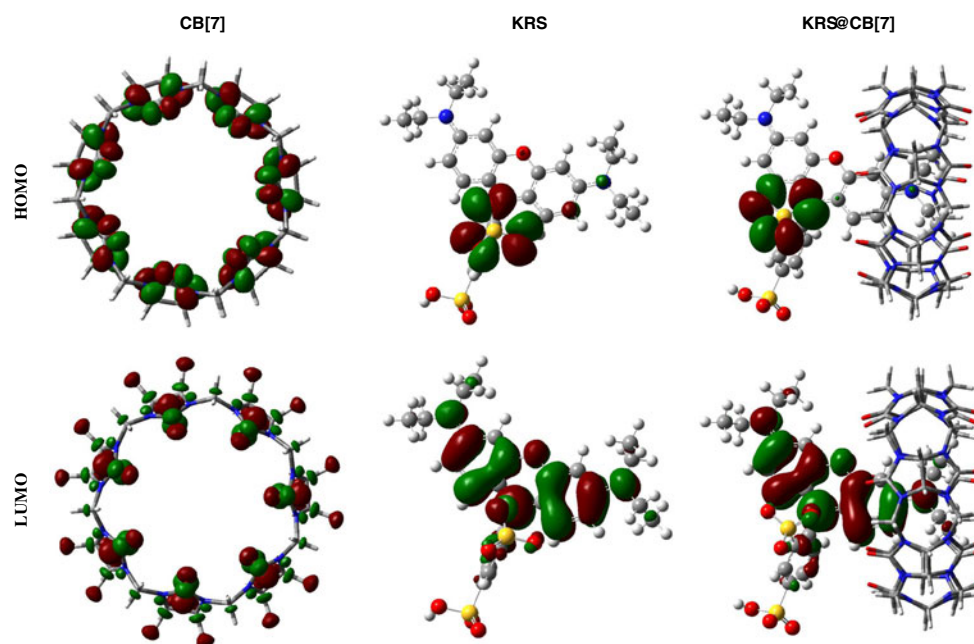
Fig. 5 Frontier orbitals of CB [7], KRS, and KRS@CB[7]

isolated hosts and guests using the GIAO method within SCRF-PCM framework of theory. In Table 4, calculated δ_H values for RhB, CB[7], and the RhB@CB[7] complex (obtained using water as solvent) are presented, along with the corresponding experimental data [7, 16]. A comparison of the δ_H values obtained from the present calculations with those observed experimentally is provided in Fig. 6. This linear plot (with a correlation coefficient of 0.99) of the experimental ^{1}H NMR chemical shifts as a function of those calculated from GIAO theory suggests that, overall, the calculated ^{1}H NMR chemical shifts agrees well with those observed experimentally.

In the following, we briefly outline how complexation influences the NMR signals of the guest. On complexation,

Table 3 Net atomic charges of the O and N atoms in CB[7], RhB, KRS, RhB@CB[7], and KRS@CB[7], obtained from the molecular electrostatic potential

Atom	Charge		RhB@CB[7]	KRS@CB[7]
$O_{(CB[7])}$	−0.406	O^{int}	−0.452	−0.419
			−0.435	−0.387
			−0.379	
		$O^{non-int}$	−0.426	−0.410
$N_{(CB[7])}$	−0.302	$N^{non-int}$	−0.310	−0.306
$N_{(RhB)}$	−0.457	N^{int}	−0.507	
	−0.353	$N^{non-int}$	−0.340	
$N_{(KRS)}$	−0.353	N^{int}	−0.318	
	−0.342	$N^{non-int}$	−0.396	

O^{int} interacting oxygens, $O^{non-int}$ average value for noninteracting oxygens, N^{int} interacting nitrogens, $N^{non-int}$ average value for noninteracting nitrogens

the protons H_g, H_d, and H_e of RhB exhibit deshielding, with the corresponding δ_H values being 8.64, 7.96, and 8.14 ppm in the calculated spectra, respectively; the signal from the H_f proton is, however, unaffected. This agrees well with the experimental spectra, where deshielding of the aromatic protons (H_g, H_d) was observed. Note that the protons H_c and H_c' in the xanthene of isolated RhB are equivalent. The H_c proton that points towards the host portal exhibits more deshielding (δ_H 7.91 ppm) than the noninteracting H_c' (δ_H 7.43 ppm). On the other hand, the H_b proton encapsulated within the host cavity is shielded on complexation. Likewise, the NMR signal from the H_b' proton (equivalent to H_b in the isolated guest) moves upfield in RhB@CB[7] complex. The δ_H signal (at 6.15 ppm) of the proton (H_a) midway between the nitrogens of adjacent glycourils is also worth noting. A broad signal near 6.60 ppm in the experimental ^{1}H NMR spectrum of RhB@CB [7] results from the overlap of individual signals from the H_b, H_b', H_a, and H_a' protons.

It was previously inferred that the complexation of cucurbituril with a laser dye can be understood by following the changes in the ^{1}H NMR signals from methyl and methylene protons. Thus, the average δ_H values for the interacting and noninteracting methylene protons of the *N,N*-diethylamino group in the RhB@CB[7] complex were predicted to be 3.19 ppm and 3.58 ppm, respectively. Moreover, a δ_H signal at 1.20 ppm arises from the shielding of interacting methyl protons, while the δ_H signal at 1.29 ppm derives from noninteracting ones. These inferences are in accord with broad upfield signals observed experimentally that are attributed to the overlap of methylene and methyl proton signals. As far as the protons on the host are concerned, the methine proton (H2) signals (δ_H=5.10 ppm) are almost unchanged

Table 4 NMR chemical shifts (δ_H, in ppm) for CB[7], RhB, KRS, RhB@CB[7], and KRS@CB[7] (1:1) complexes in water

	CB[7]		RhB		RhB@CB[7]		KRS		KRS@CB[7]	
	Present work	From [16]	Present work	From [7]	Present work	From [7]	Present work	From [8]	Present work	From [8]
H1	3.84	4.29			3.83				3.93	
H2	5.08	5.60			5.10				5.00	
H3	5.91	5.91			5.84				5.63	
H_g			8.51	8.10	8.64					
H_e			8.06	7.70	8.14	7.60	8.08	8.00	8.08	7.98
H_f			8.01		8.01	8.20	8.30	8.30	8.61	8.33
H_d			7.51	7.40	7.96	7.50	7.40	7.50	8.07	7.54
H_c			7.07	7.00	7.91	7.10	7.59	6.90	7.74	7.01
$H_c{'}$			7.07	7.00	7.43	7.10			7.35	
H_b			7.13	6.70	6.45	6.60	6.90	6.80	6.45	6.82
$H_b{'}$			7.13	6.70	7.04	6.60			6.91	
H_a			6.85	6.50	6.15	6.60	6.84	6.70	6.40	6.45
$H_a{'}$			6.85		6.99		6.84		7.34	
CH_2			3.61	3.50	3.19[a]	3.49	3.55	3.40	3.10[a]	3.15
					3.58[b]				3.57[b]	3.50
CH_3			1.30	1.10	1.20[a]	1.08	1.25	1.10	1.01[a]	0.45
					1.29[b]	0.70			1.29[b]	1.20

[a] Average δ_H for protons from the *N,N*-diethylamino group encapsulated within CB[7]

[b] Average δ_H for protons of the noninteracting *N,N*-diethylamino group

upon complexation. The H3 protons, directed toward the portals of CB[7], yield a signal at 5.84 ppm.

The ^{1}H NMR chemical shifts of isolated KRS and the KRS@CB[7] complex predicted from B3LYP calculations are compared with their correspnding experimental values [8] in Table 4. Deshielding of the aromatic protons (H_f and H_d) with δ_H signals at 8.61 and 8.07 ppm, respectively, is immediately noticeable for KRS@CB[7], as this group excludes itself from the cavity. The experimentally observed ^{1}H NMR spectrum [8] also shows deshielding (~0.04 ppm)

for these protons. However, calculations indicate that the H_e proton remains unchanged after complexation.

It is clear from Table 4 that the xanthene proton (H_b) encapsulated within the cavity of CB[7] presents a shielded signal at δ_H 6.45 ppm, while the signal due to the noninteracting $H_b{'}$ (δ_H 6.91 ppm) remains unchanged. The experimental NMR spectrum exhibits a broad signal near to 6.82 ppm for these protons. Shielding of the H_a proton (~0.44 ppm; $\delta_H=$ 7.03 ppm) encapsulated in the CB[7] cavity was also predicted. In accord with this, the experimental NMR spectrum indicated

Fig. 6 A plot of experimental δ_H values vs. ^{1}H NMR chemical shifts obtained from GIAO for CB[7], RhB, KRS, RhB@CB[7], and KRS@CB[7]
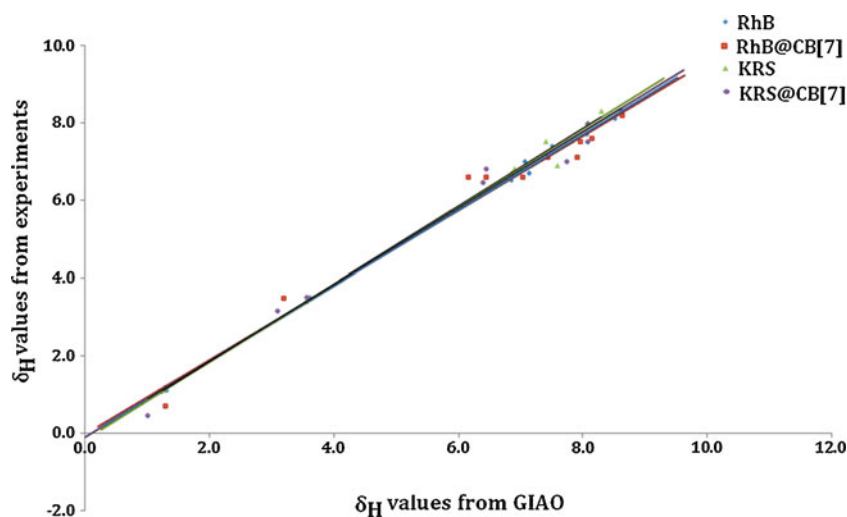
the shielding of H_a by ~0.25 ppm. The H_a' proton that points towards the host portals is deshielded; δ_H is 7.34 ppm. The methylene protons of the guest encapsulated within the cavity of the host show upfield signal at the $\delta_H =$ 3.10 ppm, while those remaining outside the cavity exhibit marginal (~0.02 ppm) deshielding compared to the NMR signal at 3.55 ppm in isolated KRS. These inferences are consistent with the experimental ^{1}H NMR spectrum, in which signals near to 3.15 ppm and 3.50 ppm are observed; the broadening of these signals can be attributed to the dynamic nature of the host–guest system in solution. A signal near to 1.01 ppm in the calculated spectrum corresponds to methyl protons of the guest encapsulated within the cavity of CB[7]; the methyl protons of the group remaining outside the cavity are merely deshielded (~0.04 ppm) compared to their value (1.25 ppm) in isolated KRS. This agrees well with the broad peaks at 0.45 and 1.20 ppm observed experimentally due to shielding and deshielding of methyl protons. Thus, the chemical shifts of the complexes are in accord with those seen in the experimental ^{1}H NMR spectra.

Conclusions

The binding patterns of RhB and KRS guests to CB[7] host were analyzed at the B3LYP/6-31G(d,p) level of theory. Both complexes (RhB@CB[7] and KRS@CB[7]) show encapsulation of one of the N,N-diethylamino groups within the CB[7] cavity, as also inferred experimentally. O–H···O and C–H···O hydrogen-bonding interactions govern the stability of the RhB@CB[7] complex. The KRS@CB[7] complex possesses only C–H···O interactions with the portals. KRS binds (178.2 kJ mol^{-1}) strongly to CB[7] than RhB (156.2 kJ mol^{-1}). Upon encapsulation within the cavity of CB[7], the interacting methylene protons of the guest molecule exhibit shielding ($\Delta\delta_H = \sim0.4$ ppm) relative to those in the isolated guest. Likewise, the methyl protons encapsulated within the cavity of CB[7] show shielding in the calculated ^{1}H NMR spectra. The trends observed for the changes in the calculated chemical shifts of the protons of the dye due to its encapsulation within the cavity of CB[7] are consistent with those seen in experimental ^{1}H NMR spectra.

References

1. Behrend R, Meyer E, Rusche F (1905) I. Über Kondensationsprodukte aus Glycoluril und Formaldehyd. Liebigs Ann Chem 339:1–37. doi:10.1002/jlac.19053390102
2. Bhasikuttan AC, Mohanty J, Nau WM, Pal H (2007) Efficient fluorescence enhancement and cooperative binding of an organic dye in a supra-biomolecular host–protein assembly. Angew Chem Int Ed Engl 46:4120–4122. doi:10.1002/anie.200604757
3. Liu Y, LI CJ, Guo DS, Pan ZH, Li Z (2007) A comparative study of complexation of β-cyclodextrin, calix[4]arenesulfonate and cucurbit[7]uril with dye guests: fluorescence behavior and binding ability. Supramol Chem 19:517–523. doi:10.1080/10610270601145444
4. Marquez C, Hung F, Nau WM (2004) Cucurbiturils: molecular nanocapsules for time-resolved fluorescence-based assays. IEEE Trans Nanobiosci 3:39–45. doi:10.1109/TNB.2004.824269
5. Nau WM, Mohanty J (2005) Taming fluorescent dyes with cucurbituril. Int J Photoenergy 7:133–141. doi:10.1155/S1110662X05000206
6. Arunkumar E, Forbes CC, Smith BD (2005) Improving the properties of organic dyes by molecular encapsulation. Eur J Org Chem 19:4051–4059. doi:10.1002/ejoc.200500372
7. Halterman RL, Moore JL, Yakshe KA, Halterman JAI, Woodson KA (2010) Inclusion complexes of cationic xanthene dyes in cucurbit[7]uril. J Incl Phenom Macrocycl Chem 66:231–241. doi:10.1007/s10847-009-9615-9
8. Mohanty J, Jagtap K, Ray AK, Nau WM, Pal H (2010) Molecular encapsulation of fluorescent dyes affords efficient narrow-band dye laser operation in water. Chem Phys Chem 11:3333–3338. doi:10.1002/cphc.201000532
9. Pinjari RV, Khedkar JK, Gejji SP (2010) Cavity diameter and height of cyclodextrins and cucurbit[n]urils from the molecular electrostatic potential topography. J Incl Phenom Macrocycl Chem 66:371–380. doi:10.1007/s10847-009-9657-z
10. Pinjari RV, Gejji SP (2008) Electronic structure, molecular electrostatic potential, and NMR chemical shifts in cucurbit[n]urils ($n=5–8$), ferrocene, and their complexes. J Phys Chem A 112:12679–12686. doi:10.1021/jp807268v
11. Frisch MJ, Trucks GW, Schlegel HB, Scuseria GE et al (2009) Gaussian 09. Gaussian Inc., Wallingford
12. Becke AD (1993) Density-functional thermochemistry. III. The role of exact exchanges. J Chem Phys 98:5648–5652. doi:10.1063/1.464913
13. Lee C, Yang W, Parr RG (1988) Development of the Colle–Salvetti correlation-energy formula into a functional of the electron density. Phys Rev B 37:785–789. doi:10.1103/PhysRevB.37.785
14. Wolinski K, Hilton JF, Pulay P (1990) Efficient implementation of the gauge-independent atomic orbital method for NMR chemical shift calculations. J Am Chem Soc 112:8251–8260. doi:10.1021/ja00179a005
15. Mierts S, Scrocco E, Tomasi J (1981) Electrostatic interaction of a solute with a continuum. A direct utilization of ab initio molecular potentials for the prevision of solvent effects. J Chem Phys 55:117–129. doi:10.1016/0301-0104(81)85090-2
16. Kim J, Jung IS, Kim SY, Lee E, Kang JK, Sakamoto S, Yamaguchi K, Kim K (2000) New cucurbituril homologues: syntheses, isolation, characterization, and X-ray crystal structures of cucurbit[n]uril ($n=5$, 7, and 8). J Am Chem Soc 122:540–541. doi:10.1021/ja993376p
17. Pinjari RV, Joshi KA, Gejji SP (2007) Theoretical studies on hydrogen bonding, NMR chemical shifts and electron density topography in α,β,γ-cyclodextrin conformers. J Phys Chem A 111:13583–13589. doi:10.1021/jp074539w